Optical Pumping of vaporized ^{85}Rb and ^{87}Rb

Igal Press
Department of Physics, University of Winnipeg, Winnipeg, Manitoba R3B 2E9
(Dated: April 20, 2023)

Optical pumping is the process where 795 nm light is used to "pump" ^{85}Rb and ^{87}Rb to higher spin states. The experiment is used to examine several topics such as the effects of zero-field transitions, low-field resonances (LFR), and Quadratic Zeeman splitting in the naturally occurring ^{85}Rb and ^{87}Rb isotopes. The zero-field transitions were found to be when the horizontal sweep field was set to 34.2 μT, and the ratio between frequency to current flowing in the horizontal Helmholtz coils between ^{85}Rb and ^{87}Rb to be 1.493(2) with a theoretical value of 1.5.

I. INTRODUCTION

A. The history of optical pumping

Optical pumping was first theorized in 1950 by A. Kastler, and experimentally realized by T.H. Maiman in 1960 and is now widely used for high frequency spectroscopy, exploring atomic energy states, probing spin state transitions, and is a useful pedagogical tool to teach students the practical applications of quantum mechanics in a lab setting [1]-[4].

B. Why Rubidium, and its usefulness in optical pumping

The Rubidium atom was chosen to be used in its natural states, ^{85}Rb, and ^{87}Rb due to its being an alkali metal with one valence electron, and vaporization ability [1]-[3]. Having one valence electron allows the Rubidium atom to be viewed as a Hydrogen replacement due to the practicality of theoretically simplifying the structure into that of an exactly solvable Hydrogen atom. The Hydrogen atom is a useful pedagogical tool due to its simple nature of having one electron, and one proton in its most common isotope $^1_1$H, and simplifying the Rubidium structure to that of $^1_1$H allows useful theoretical knowledge learned in a classroom setting to be carried over into a practical lab setting.

Optical pumping is a process that raises atoms to higher internal energy states by increasing the value of spin using polarized light. 795 nm right circularly polarized light was used to pump atoms into the higher quantum spin state M = +2. Rubidium came in two forms for this experiment: the ground state and the first excited state (^{2}S$_{1/2}$, ^{2}P$_{1/2}$), these states were further split into hyperfine splitting, and then into Zeeman splitting using an external weak magnetic field [2]-[7].

The half-integer spin caused by the singular valence electron causes this system to be a doublet system with a multiplicity of 2 which will allow for analysis into double quantum transition of the Rubidium further into the experiment [3].

II. THEORY

A. Use of Alkali metals to view Rubidium as a Hydrogen replacement

Alkali metals have the unique property of having one valence electron making them both highly reactive, and easily simplified to a Hydrogen model. The Rubidium atom was chosen specifically for this quality, coming in the electron configuration:

$$1s^2 2s^2 2p^6 3s^2 3p^6 3d^{10} 4s^2 4p^6 5s$$

Where the full, inner electron shells can be disregarded and viewed as un-reactive in the approximations that will be used [2].

The valence electron can be described as having non-nuclear spin, as in the spin is not including the nucleus of the Rubidium atom. This spin can be defined by its orbital angular momentum, L, and spin angular momentum, S, with a total non-nuclear angular momentum of J all evaluated in units of $\hbar$ [2]. These different spins can be evaluated in terms of the relation $\vec{J} = \vec{L} + \vec{S}$ where J is typically constant. In the ground state of Hydrogen - which can be extended to Rubidium - the orbital angular momentum L = 0, giving the total non-nuclear angular momentum a value of J = $1/2\hbar$. This can be extended to the first excited state giving rise to the ^{2}P$_{1/2}$ and ^{2}S$_{1/2}$ states that'll be used in this experiment.

When the nuclear spin, denoted I, is factored in, the total angular momentum of the atom becomes a new symbol F$\in Z$, where $\vec{F} = \vec{I} \pm \vec{J}$ and further splits the fine structure into the hyperfine structure. Where Zeeman splitting can be further observed [2] [5]. The total nuclear magnetic spin found in the ^{2}P$_{1/2}$ and ^{2}S$_{1/2}$ states are $\vec{I} = 3/2\hbar$, where $\vec{J} = 1/2\hbar$ leading to the F = 1, 2 levels seen in hyperfine splitting.

B. Quantum numbers and their relation to photon absorption and Zeeman splitting

Quantum numbers come in two variations in this experiment, F states, and M states, where M can be any

number between -F→+F. The F quantum state is described by the hyperfine splitting and can have values of 1, or 2, while M states describe Zeeman splitting and can be seen in Fig. 1.

Photons carry integer angular momentum as well, where right-handed circularly polarized light σ_+ carries angular momentum +1, left-handed circularly polarized light σ_- carries an angular momentum of -1, and linearly polarized light π has 0 total angular momentum [6]. When σ_+ light gets absorbed by the Rubidium, they act as raising operators to the system increasing the M value by 1, and "raising it up" a spin state [3]. After a very short amount of time, ≈1-5 ms, the light gets re-emitted with either a π, σ_+ or σ_- polarization [2] [3]. When linearly polarized light gets re-emitted, they carry with them 0 spin and leaving the M state permanently raised. After ≈10-20 ms the spin states get raised and lowered enough times during the pumping time that they will eventually all be raised into the M = 2 level, where they will remain [2] [7]. Once the spin states reach M = 2 they will be unable to absorb light due to the fact that M can only be integers between ±F and the light will pass through the vaporized Rubidium sample without interacting. These processes can be viewed pictorially in Fig. 1.

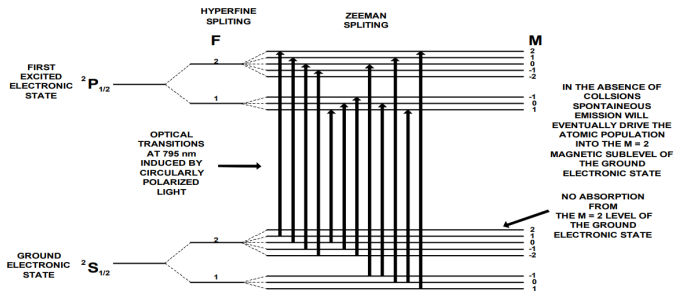

FIG. 1: A diagram of hyper-fine and Zeeman splitting displaying the total angular momentum of the ^{87}Rb atom detailing the angular momentum quantum number F, and the magnetic quantum number M, image sourced from Ref [2]

C. Rubidium in a magnetic field, and finding a zero-field transition

The magnetic field in the optical pumping experiment is caused by four Helmholtz coils, two in vertical parallel, and two in horizontal parallel. These Helmholtz coils are meant to cancel the magnetic field of the Earth ($|\vec{B}_e|$) and allow our experiment to function inside of a net-zero magnetic field. As the horizontal magnetic field is swept, it'll reach a point called the zero-field transition, where the magnetic field is swept from negative to positive eventually crossing through the zero point where the total magnetic field is zero between the coils [2]. As the horizontal magnetic field is swept the transmitted light seen in the photo-diode decreases to zero at the zero-field transition, eventually increasing back to the maximum value as the magnetic field increases further from the zero.

It's important to note that at the zero-field the energy levels in Rubidium become degenerate and the M sublevels needed for Zeeman splitting converge allowing all the light to be absorbed by the Rubidium [2]. This is the reason that as the horizontal field is swept through zero, the transmitted light intensity decreases increasingly [5]. The zero-field transition isn't the only magnetic field level where the M states converge and become degenerate, and this can be seen in Fig. 5.

III. METHOD

A. Equipment setup and description

The experimental setup is loosely detailed in Fig. 2, where it can be seen that a Rubidium RF discharge lamp was used to emit 780 nm and 795 nm wavelength light at the sample while passing through several polarizers of different orientations, and an interference filter [1] [2]. For optical pumping of Rubidium, the 780 nm light had to be filtered out, and to do this an interference filter that acted as both a high-pass and a low-pass filter was used to filter out any light that wasn't ≈795 nm, and the before and after results of the implementation of the interference filter can be seen in Fig. 3.

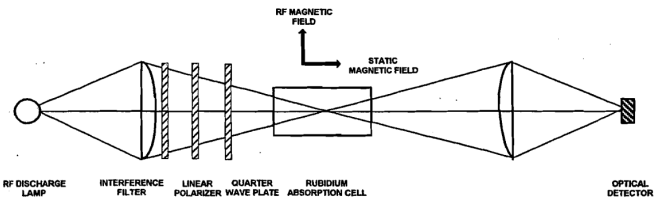

FIG. 2: The experimental setup for optical pumping with the RF magnetic field present for the low-field resonance and high-field resonance experiment. Ref [2].

To prevent the light from diverging before it interacted with the sample, a convex lens was used to stabilize the light so that the light would become parallel relative to itself so that there would be an even distribution of light throughout the Rubidium absorption cell. After passing through the convex lens, the light would pass through a linear polarizer before passing through a quarter-wave plate circular polarizer to give the light a total angular momentum of M = +1 [2]. After converging at the Rubidium absorption cell the light would diverge again before passing through a second convex lens which would converge the light to be registered as a signal by the photodiode.

It's important to note that the photodiode takes the time average intensity of the light passing through, and

as such it does not have the ability to differentiate based on polarization state.

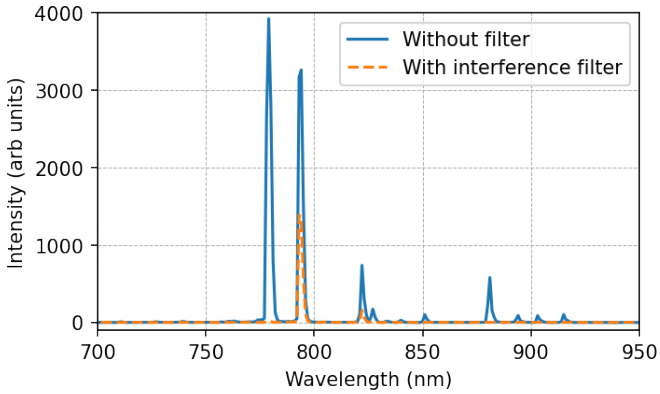

FIG. 3: Light is emitted by the RF discharge lamp with wavelengths 780 nm and 795 nm. The 780 nm light is removed with the interference filter only allowing the 795 nm light to pass through the filter to be polarized [2].

The apparatus was outfitted with four Helmholtz coils, two in vertical parallel, and two in horizontal parallel of different dimensions and coil turns. Some selected information about the Helmholtz coils can be seen in Table I. The Rubidium absorption cell would be heated to 323.2 K using equipment supplied by TeachSpin to heat the Rb and allow it to homogenize with the Ne buffer gas [2]. A black cloth shroud was draped over the experiment during data acquisition so as to mitigate light pollution in the data. More information about the equipment regarding physical dimensions and its specs/accessories can be found in Ref [1] and a more detailed experimental setup can be found in Section 3 of Ref [2].

	Mean Radius (cm)	Turns/side	Field/Amp (Tx10^{-4}/Amp
Vertical Field	11.735	20	1.5
Horizontal Field	15.79	154	8.8
Sweep Field	16.39	11	0.60

TABLE I: Description of the vertical and horizontal Helmholtz coils. Sourced from Ref [2]

B. Variation of the $\vec{B}$ field to create a Zero-field transition

The magnetic field surrounding the Rubidium absorption cell could be adjusted through the increase or decrease of the current flowing through the Helmholtz coils which could be selectively altered through use of the vertical and horizontal sweep knobs on the PID controller. The table holding the setup for the optical pumping equipment was adjusted to be aligned with magnetic North of the Earth's magnetic field

The oscilloscope was set to XY mode with persistence set to 100% so as to track the movement patterns of the data point as it moved through the magnetic field as the vertical and horizontal magnetic fields were modified. The vertical field knob was then swept until the data point reached a maximum, while also remaining at a minimal distance from the zero-field transition. It's possible to see the process in the various vertical field sweep trials in Fig. 4.

When the vertical field was determined to be at the ideal current, the horizontal field was swept through slowly until a peak was found which was then labelled the zero-field transition. The values of currents flowing through the vertical and horizontal Helmholtz coils were then recorded using a multi-meter attached to the PTD controller. After the values were recorded, Table I could be used to calculate the magnetic field of the Earth's strength, $|\vec{B}_e|$. Several other measurements with varying increasing and decreasing currents running through the vertical Helmholtz coil were also taken and can be seen in Fig. 4.

A function generator was set to 150 kHz in preparation of finding the low-field resonance of the ^{85}Rb and ^{87}Rb isotopes. The sweep field for the horizontal Helmholtz coil was adjusted to increase the current until the resonant frequency of the specific isotope was reached. This resonant frequency is determined by the formula

$$\nu_H = g_f \mu_0 B/h \tag{1}$$

$$B = \mu_0 N I/2r \tag{2}$$

where ν_H is the frequency related to the Zeeman splitting energy set by B [2]. When $\nu_H = \nu_{Function}$, the low-field resonance is achieved which can be seen in Fig. 5.

C. The Quadratic Zeeman Effect

To explore the Quadratic Zeeman Effect, the radio-frequency gain (RF gain) must be increased to 3, and 10x gain, and the frequencies of the function generator are 4.9874 MHz for ^{87}Rb and 3.3391 MHz for ^{85}Rb. This will allow precision movement between the Zeeman levels where the difference between the energy levels is less than 10^{-8} ev [3]. The Horizontal Sweep is set to the center of the resonant frequencies of the ^{85}Rb and ^{87}Rb, where the gain is then turned up to the desired value. Once the gain is increased, the Horizontal Sweep will be slowly turned to view the resonances between Zeeman levels. Due to

the fact that this is a doublet system, when the gain is increased to 10x a second set of resonances can be seen which are known as double quantum transitions.

IV. RESULTS AND DISCUSSION

A. Zero-field transitions and Low-field resonances

It was found that to cancel the vertical component of the Earth's magnetic field, 0.228 A or 34.2 μT must be induced in the vertical Helmholtz coil This can be seen in Fig. 4 where the condition for vertical field cancellation (black curve) is re-plotted in all subfigures.

In Figure 4a the vertical Helmholtz field was changed to increase current to 0.235 A (orange), and 0.244 A (purple) showing a respective magnetic field increase in the vertical Helmholtz coil to 35.25 μT and 36.6 μT. Similarly, in Figure 4b the vertical Helmholtz coil had decreasing current from 0.220 A to 0.215 A with a corresponding field shift of 33.0 μT and 32.25 μT.

In Figure 4c the apparatus was kept with a constant vertical Helmholtz field strength of 34.2 μT with an apparatus offset alignment with respect to the Earth's magnetic field of $\pm 10°$.

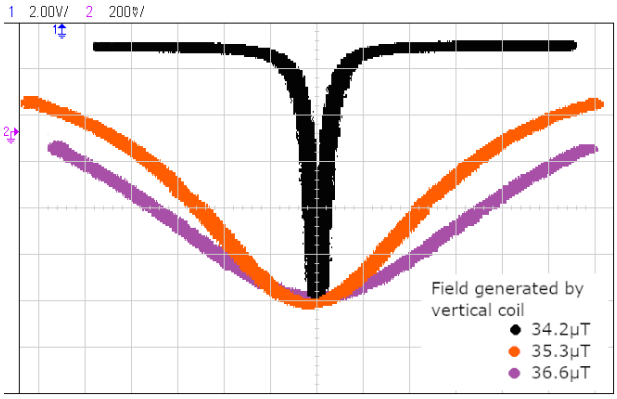

(a) Zero-field transitions with increasing current in the vertical Helmholtz coils.

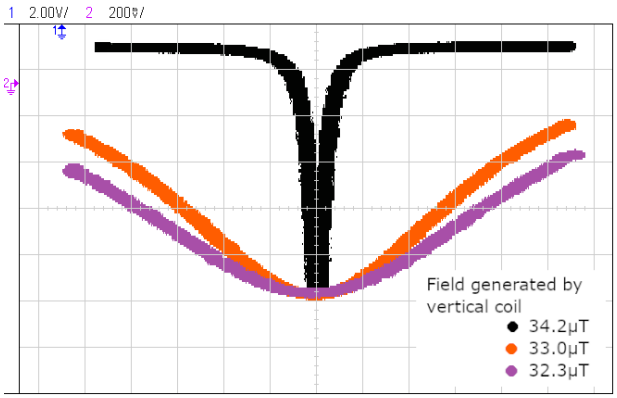

(b) Zero-field transitions with decreasing current in the vertical Helmholtz coils.

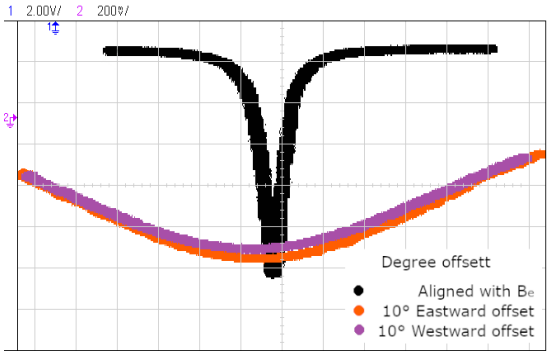

(c) Zero-field transitions with a constant $\vec{B}$ field, but an offset of the apparatus 10° Eastwards and Westwards.

FIG. 4: Zero-field transitions of ^{87}Rb and ^{85}Rb with changing current in the vertical Helmholtz coils (a)(b), and apparatus offset from alignment of $\vec{B_e}$ (c).

To find the Low-field resonances of ^{85}Rb and ^{87}Rb seen in Fig. 5 the function generator as set to a sinusoidal frequency of 25 Hz with a vertical magnetic field strength of 34.2 μT. The current in the horizontal field sweep was increased until the resonant frequencies of the Rubidium was visible where the current value at the LFR point would be taken. The function generator had increasing frequency in increments of 25 Hz with LFR current measurements being taken for ^{85}Rb and ^{87} for each frequency.

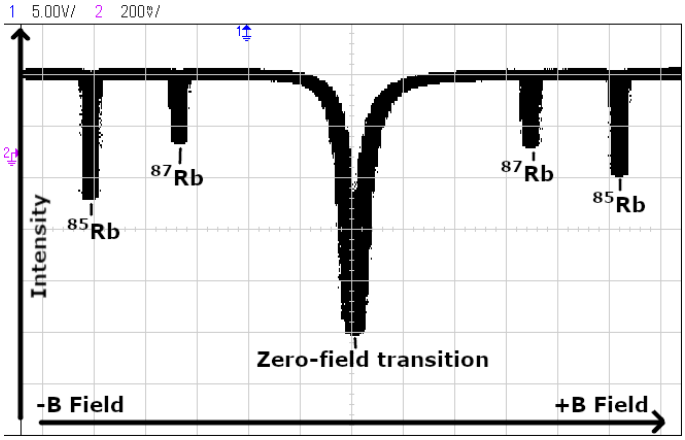

FIG. 5: The magnetic field causing the zero-field transition where the ^{87}Rb and ^{85}Rb atoms were all in the $m_l = +2$ state, and where the ^{85}Rb and ^{87}Rb were individually in the $m_l = +2$ state.

Over 9 trials the slope of the current running in the horizontal sweep coil vs. frequency outputted by the function generator yielded a result where the slope of ^{85}Rb was found to be $\text{slope}_{85} = 3.455(1)$ and the slope of ^{87}Rb was $\text{slope}_{87} = 2.309(1)$. The ratio of slope_{87} / slope_{85} was found to be 1.493(2) with an expected ratio of 1.5 yielding a 0.4(1)% difference in experimental to theoretical values seen in Fig. 6.

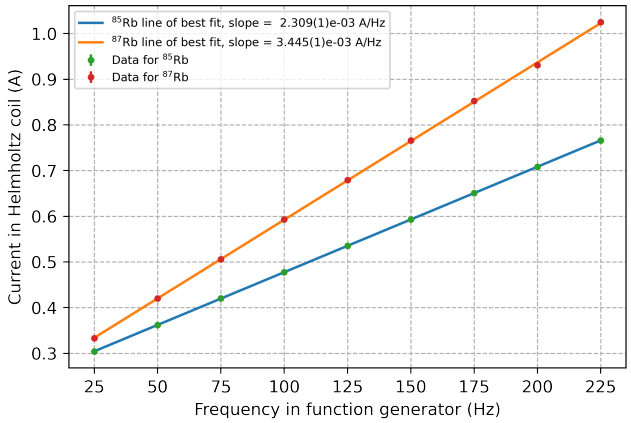

FIG. 6: Current in the Helmholtz coils relative to the frequency in the function generator creating a low-field RF transition for ^{87}Rb and ^{85}Rb. The slopes in A/Hz for ^{87}Rb and ^{85}Rb were found to be $2.309(1) \times 10^{-3}$ and $3.455(1) \times 10^{-3}$ respectively, with a ratio of slope_{87} / $\text{slope}_{85} = 1.493(2)$ with an expected ratio of 1.5

B. Zeeman splitting of the ^{87}Rb and ^{85}Rb

The gain was increased to 3x to observe Zeeman splitting as seen in Figures 7a and 7c, and 10x to observe quadratic Zeeman splitting in Figures 7b and 7d. Zeeman splitting in ^{85}Rb can be viewed in Figures 7a and 7b, whereas Zeeman splitting in ^{87}Rb can be viewed in 7c and 7d.

When viewing the quadratic Zeeman splitting in Figures 7b and 7d it's possible to see the double quantum transitions between each Zeeman peak. The ^{85}Rb also appears to have two extra Zeeman peaks compared to the ^{87}Rb, and 4 extra quadratic Zeeman peaks.

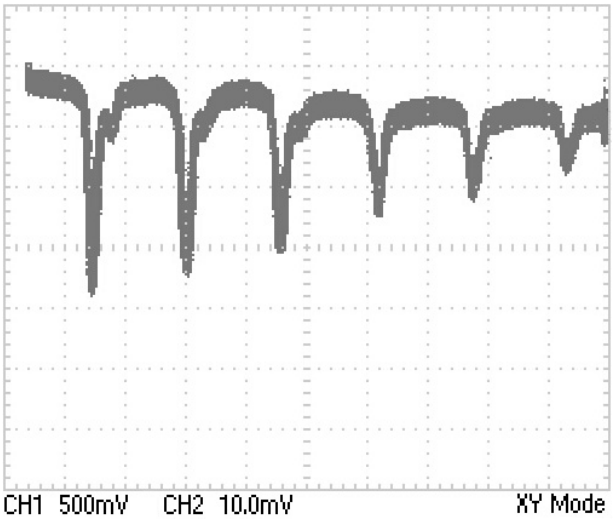

(a) Zeeman splitting of an ^{85}Rb atom with an RF gain = 3.

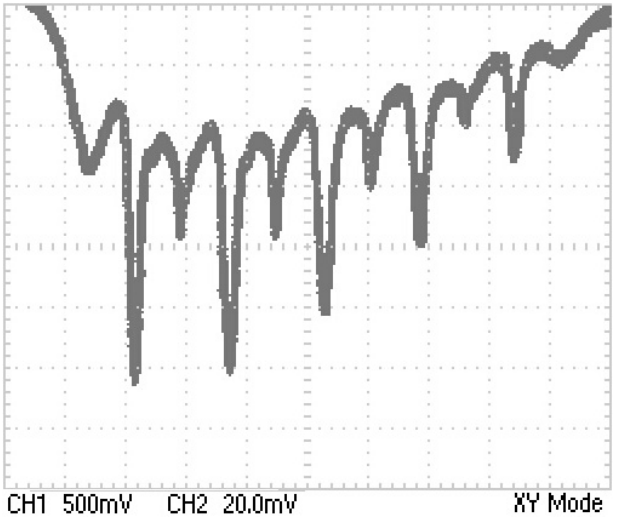

(b) Zeeman splitting displaying double quantum transitions in ^{85}Rb with an RF gain = 10.

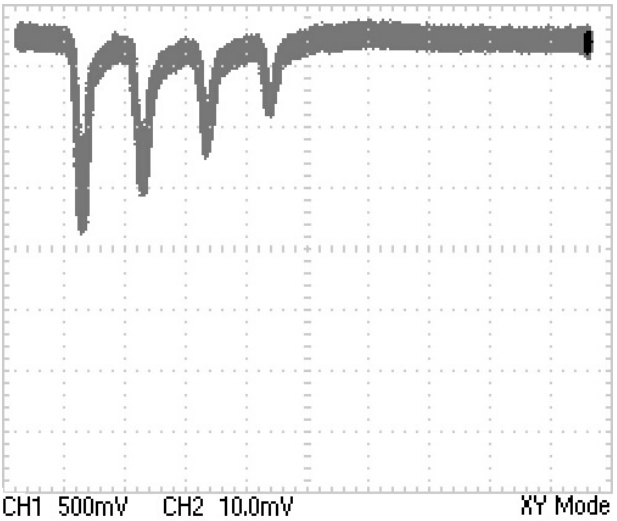

(c) Zeeman splitting of an ^{87}Rb atom with an RF gain = 3.

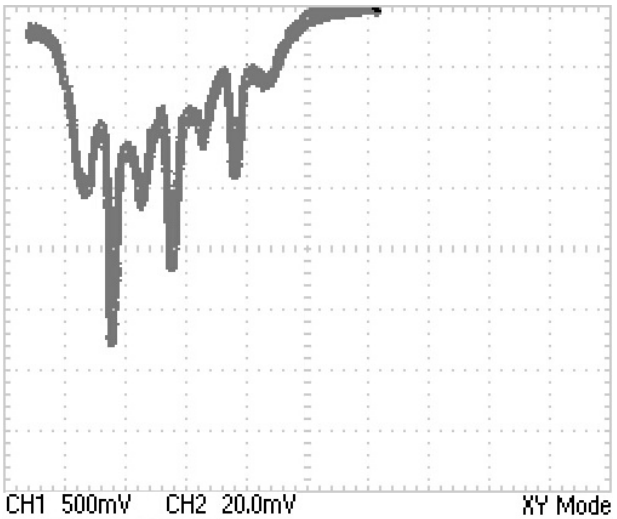

(d) Zeeman splitting displaying double quantum transitions in ^{87}Rb with an RF gain = 10.

FIG. 7: Zeeman splitting in ^{85}Rb and ^{87}Rb atoms.

V. CONCLUSION

The Rubidium was successfully optically pumped with 795 nm σ_+ light carrying a +1 angular momentum to increase the M values of all the Rubidium in the Rubidium absorption cell to the maximum value of M = 2. The current induced into the vertical Helmholtz coil to cancel the vertical component of the Earth's magnetic field was found to be 0.228 A or 34.2 μT. Low-field resonance was measured over several trials between ^{85}Rb and ^{87}Rb where the ratio taken between the slopes of their current/frequency was found to be 1.493(2) with an expected ratio of 1.5 with a 0.4(1)% difference between experimental and theoretical values. Non-quadratic as well as quadratic Zeeman splitting were also observed by using 3 and 10x RF gain respectively where the number of peaks seen in non-quadratic Zeeman splitting for ^{85}Rb was 6, while for ^{87}Rb 4 peaks were seen. When quadratic Zeeman splitting is observed for 10x RF gain, 11 peaks were seen in ^{85}Rb and 7 peaks in ^{87}Rb.

[1] Optical Pumping — TeachSpin. (n.d.). Retrieved February 4, 2023, from https://www.teachspin.com/optical-pumping

[2] Optical Pumping of Rubidium, Guide to the Experiment.

[3] Recht, J., Klein, W. (n.d.). Optical pumping of Rubidium. Retrieved February 4, 2023, from https://www.physics.wisc.edu/courses/home/spring2020/407/experiments/opticalpumping/opticalpumping.pdf

[4] Boudrioua, A., Chakaroun, M., Fischer, A. (n.d.). An Introduction to Organic Lasers. Science Direct. Retrieved from https://www.sciencedirect.com/book/9781785481581/an-introduction-to-organic-lasers.

[5] Bailey, D. (n.d.). Optical Pumping in Rubidium. Retrieved February 4, 2023, from https://www.physics.utoronto.ca/~phy326/rb/rb.pdf

[6] Hyperfine Structure. (2018, January 27). Retrieved February 4, 2023, from https://chem.libretexts.org/Bookshelves/Physical_and_Theoretical_Chemistry_Textbook_Maps/Supplemental_Modules_(Physical_and_Theoretical_Chemistry)/Quantum_Mechanics/13%3A_Fine_and_Hyperfine_Structure/Hyperfine_Structure

[7] Wang, E. Optical Pumping of Rubidium Vapor. Retrieved February 2, 2023, from http://web.mit.edu/wangfire/pub8.14/oppaper.pdf